

## Measurement of the $^{244}\text{Cm}$ and $^{246}\text{Cm}$ neutron-induced capture cross sections at the n\_TOF facility

V. Alcayne<sup>1</sup>, A. Kimura<sup>2</sup>, E. Mendoza<sup>1</sup>, D. Cano-Ott<sup>1</sup>, T. Martínez<sup>1</sup>, O. Aberle<sup>3</sup>, J. Andrzejewski<sup>4</sup>, L. Audouin<sup>5</sup>, V. Bécares<sup>1</sup>, M. Bacak<sup>3,6,7</sup>, M. Barbagallo<sup>3,8</sup>, F. Bečvář<sup>9</sup>, G. Bellia<sup>10,11</sup>, E. Berthoumieux<sup>7</sup>, J. Billowes<sup>12</sup>, D. Bosnar<sup>13</sup>, A. Brown<sup>14</sup>, M. Busso<sup>8,15,16</sup>, M. Caamaño<sup>17</sup>, L. Caballero-Ontanaya<sup>18</sup>, F. Calviño<sup>19</sup>, M. Calviani<sup>3</sup>, A. Casanovas<sup>19</sup>, F. Cerutti<sup>3</sup>, Y. H. Chen<sup>5</sup>, E. Chiaveri<sup>3,12,20</sup>, N. Colonna<sup>8</sup>, G. Cortés<sup>19</sup>, M. A. Cortés-Giraldo<sup>20</sup>, L. Cosentino<sup>10</sup>, S. Cristallo<sup>8,15,21</sup>, L. A. Damone<sup>8,22</sup>, M. Diakaki<sup>23,3</sup>, M. Dietz<sup>24</sup>, C. Domingo-Pardo<sup>18</sup>, R. Dressler<sup>25</sup>, E. Dupont<sup>7</sup>, I. Durán<sup>17</sup>, Z. Eleme<sup>26</sup>, B. Fernández-Domínguez<sup>17</sup>, A. Ferrari<sup>3</sup>, P. Finocchiaro<sup>10</sup>, V. Furman<sup>27</sup>, K. Göbel<sup>28</sup>, A. Gawlik<sup>4</sup>, S. Gilardoni<sup>3</sup>, T. Glodariu<sup>29</sup>, I. F. Gonçalves<sup>30</sup>, E. González-Romero<sup>1</sup>, C. Guerrero<sup>20</sup>, F. Gunsing<sup>7</sup>, H. Harada<sup>2</sup>, S. Heinitz<sup>25</sup>, J. Heyse<sup>31</sup>, D. G. Jenkins<sup>14</sup>, F. Käppeler<sup>32</sup>, Y. Kadi<sup>3</sup>, T. Katabuchi<sup>33</sup>, N. Kivel<sup>25</sup>, I. Knapova<sup>9</sup>, M. Kokkoris<sup>23</sup>, Y. Kopatch<sup>27</sup>, M. Krčička<sup>9</sup>, D. Kurtulgil<sup>28</sup>, I. Ladarescu<sup>18</sup>, C. Lederer-Woods<sup>24</sup>, J. Lerendegui-Marco<sup>20</sup>, S. Lo Meo<sup>34,35</sup>, S. J. Lonsdale<sup>24</sup>, D. Macina<sup>3</sup>, A. Manna<sup>35,36</sup>, A. Masi<sup>3</sup>, C. Massimi<sup>35,36</sup>, P. Mastinu<sup>37</sup>, M. Mastromarco<sup>3</sup>, F. Matteucci<sup>38,39</sup>, E. A. Maugeri<sup>25</sup>, A. Mazzone<sup>8,40</sup>, A. Mengoni<sup>34</sup>, V. Michalopoulou<sup>23</sup>, P. M. Milazzo<sup>38</sup>, F. Mingrone<sup>3</sup>, A. Musumarra<sup>10,11</sup>, A. Negret<sup>29</sup>, R. Nolte<sup>41</sup>, F. Ogállar<sup>42</sup>, A. Oprea<sup>29</sup>, N. Patronis<sup>26</sup>, A. Pavlik<sup>43</sup>, J. Perkowski<sup>4</sup>, L. Persanti<sup>8,15,21</sup>, I. Porras<sup>42</sup>, J. Praena<sup>42</sup>, J. M. Quesada<sup>20</sup>, D. Radeck<sup>41</sup>, D. Ramos-Doval<sup>5</sup>, T. Rauscher<sup>44,45</sup>, R. Reifarth<sup>28</sup>, D. Rochman<sup>25</sup>, M. Sabaté-Gilarte<sup>3,20</sup>, A. Saxena<sup>46</sup>, P. Schillebeeckx<sup>31</sup>, D. Schumann<sup>25</sup>, S. Simone<sup>10</sup>, A. G. Smith<sup>12</sup>, N. V. Sosnin<sup>12</sup>, A. Stamatopoulos<sup>23</sup>, G. Tagliente<sup>8</sup>, J. L. Tain<sup>18</sup>, T. Talip<sup>25</sup>, A. Tarifeño-Saldivia<sup>19</sup>, L. Tassan-Got<sup>3,23,5</sup>, A. Tsinganis<sup>3</sup>, J. Ulrich<sup>25</sup>, S. Urlass<sup>3,47</sup>, S. Valenta<sup>9</sup>, G. Vannini<sup>35,36</sup>, V. Variale<sup>8</sup>, P. Vaz<sup>30</sup>, A. Ventura<sup>35</sup>, D. Vescovi<sup>8,15</sup>, V. Vlachoudis<sup>3</sup>, R. Vlastou<sup>23</sup>, A. Wallner<sup>48</sup>, P. J. Woods<sup>24</sup>, T. Wright<sup>12</sup>, and P. Žugec<sup>13</sup>

<sup>1</sup>Centro de Investigaciones Energéticas Medioambientales y Tecnológicas (CIEMAT), Spain

<sup>2</sup>Japan Atomic Energy Agency (JAEA), Tokai-mura, Japan

<sup>3</sup>European Organization for Nuclear Research (CERN), Switzerland

<sup>4</sup>University of Lodz, Poland

<sup>5</sup>Institut de Physique Nucléaire, CNRS-IN2P3, Univ. Paris-Sud, Université Paris-Saclay, F-91406 Orsay Cedex, France

<sup>6</sup>Technische Universität Wien, Austria

<sup>7</sup>CEA Irfu, Université Paris-Saclay, F-91191 Gif-sur-Yvette, France

<sup>8</sup>Istituto Nazionale di Fisica Nucleare, Sezione di Bari, Italy

<sup>9</sup>Charles University, Prague, Czech Republic

<sup>10</sup>INFN Laboratori Nazionali del Sud, Catania, Italy

<sup>11</sup>Dipartimento di Fisica e Astronomia, Università di Catania, Italy

<sup>12</sup>University of Manchester, United Kingdom

<sup>13</sup>Department of Physics, Faculty of Science, University of Zagreb, Zagreb, Croatia

<sup>14</sup>University of York, United Kingdom

<sup>15</sup>Istituto Nazionale di Fisica Nucleare, Sezione di Perugia, Italy

<sup>16</sup>Dipartimento di Fisica e Geologia, Università di Perugia, Italy

<sup>17</sup>University of Santiago de Compostela, Spain

<sup>18</sup>Instituto de Física Corpuscular, CSIC - Universidad de Valencia, Spain

- <sup>19</sup>Universitat Politècnica de Catalunya, Spain  
<sup>20</sup>Universidad de Sevilla, Spain  
<sup>21</sup>Istituto Nazionale di Astrofisica - Osservatorio Astronomico di Teramo, Italy  
<sup>22</sup>Dipartimento di Fisica, Università degli Studi di Bari, Italy  
<sup>23</sup>National Technical University of Athens, Greece  
<sup>24</sup>School of Physics and Astronomy, University of Edinburgh, United Kingdom  
<sup>25</sup>Paul Scherrer Institut (PSI), Villingen, Switzerland  
<sup>26</sup>University of Ioannina, Greece  
<sup>27</sup>Joint Institute for Nuclear Research (JINR), Dubna, Russia  
<sup>28</sup>Goethe University Frankfurt, Germany  
<sup>29</sup>Horia Hulubei National Institute of Physics and Nuclear Engineering, Romania  
<sup>30</sup>Instituto Superior Técnico, Lisbon, Portugal  
<sup>31</sup>European Commission, Joint Research Centre, Geel, Retieseweg 111, B-2440 Geel, Belgium  
<sup>32</sup>Karlsruhe Institute of Technology, Campus North, IKP, 76021 Karlsruhe, Germany  
<sup>33</sup>Tokyo Institute of Technology, Japan  
<sup>34</sup>Agenzia nazionale per le nuove tecnologie (ENEA), Bologna, Italy  
<sup>35</sup>Istituto Nazionale di Fisica Nucleare, Sezione di Bologna, Italy  
<sup>36</sup>Dipartimento di Fisica e Astronomia, Università di Bologna, Italy  
<sup>37</sup>Istituto Nazionale di Fisica Nucleare, Sezione di Legnaro, Italy  
<sup>38</sup>Istituto Nazionale di Fisica Nucleare, Sezione di Trieste, Italy  
<sup>39</sup>Dipartimento di Astronomia, Università di Trieste, Italy  
<sup>40</sup>Consiglio Nazionale delle Ricerche, Bari, Italy  
<sup>41</sup>Physikalisch-Technische Bundesanstalt (PTB), Bundesallee 100, 38116 Braunschweig, Germany  
<sup>42</sup>University of Granada, Spain  
<sup>43</sup>University of Vienna, Faculty of Physics, Vienna, Austria  
<sup>44</sup>Department of Physics, University of Basel, Switzerland  
<sup>45</sup>Centre for Astrophysics Research, University of Hertfordshire, United Kingdom  
<sup>46</sup>Bhabha Atomic Research Centre (BARC), India  
<sup>47</sup>Helmholtz-Zentrum Dresden-Rossendorf, Germany  
<sup>48</sup>Australian National University, Canberra, Australia

**Abstract.** The neutron capture reactions of the  $^{244}\text{Cm}$  and  $^{246}\text{Cm}$  isotopes open the path for the formation of heavier Cm isotopes and heavier elements such as Bk and Cf in a nuclear reactor. In addition, both isotopes belong to the minor actinides with a large contribution to the decay heat and to the neutron emission in irradiated fuels. There are only two previous  $^{244}\text{Cm}$  and  $^{246}\text{Cm}$  capture cross section measurements: one in 1969 using a nuclear explosion [1] and the most recent data measured at J-PARC in 2010 [2]. The data for both isotopes are very scarce due to the difficulties in performing the measurements: high intrinsic activity of the samples and limited facilities capable of providing isotopically enriched samples.

We have measured both neutron capture cross sections at the n\_TOF Experimental Area 2 (EAR-2) with three  $\text{C}_6\text{D}_6$  detectors and also at Area 1 (EAR-1) with the TAC. Preliminary results assessing the quality and limitations (background subtraction, measurement technique and counting statistics) of this new experimental datasets are presented and discussed.

## 1 Introduction

Accurate neutron capture cross section data for minor actinides (MAs) are required to estimate the production and transmutation rates of MAs in light-water reactors (LWR) with a high burnup, critical fast reactors like Gen-IV systems and other innovative devices such as

accelerator driven systems (ADS) [3]. The  $^{244}\text{Cm}$  ( $T_{1/2}=18.1$  years) and  $^{246}\text{Cm}$  ( $T_{1/2}=4730$  years) isotopes are among the most important MAs due to the difficulties in their transmutation and their contribution to the radiotoxicity of the irradiated nuclear fuels. In particular, even after three years of cooling,  $^{244}\text{Cm}$  shares nearly 50% of the total actinide decay heat in irradiated reactor fuels with a high burnup. In addition, both of them are in the path of the creation of any heavier Cm isotopes and heavier elements like Bk and Cf.

Only two previous capture measurements were done before the n\_TOF measurements. The first one, done in 1969 [1], used the neutrons produced in an under-ground nuclear explosion. The  $^{244}\text{Cm}$  (n, $\gamma$ ) cross section was measured in a range from 20 eV to 1 keV and for the  $^{246}\text{Cm}$ (n, $\gamma$ ) from 20 eV to 400 eV. The second capture measurement was performed in 2010 with a large coverage Ge-array in the Accurate Neutron Nucleus Reaction Measurement Instrument (ANNRI) at J-PARC [2]. In this second measurement the data obtained for both isotopes range from 2 eV to 300 eV. The resonance analysis was done up to 30 eV. The scarcity of the available data and the many experimental challenges involved in the two previous measurements motivated an additional measurement under different conditions, i.e., in a different facility, with different detectors and monitors and with a different methodology.

## 2 Experiment

The same samples used at J-PARC have been measured at n\_TOF. In this facility, the neutron beam is generated through spallation of 20 GeV/c protons, which are extracted in pulses from the CERN Proton Synchrotron and impinging on a lead target. The pulses have a nominal intensity of  $7\times 10^{12}$  protons and a time spread of 7 ns (rms). The neutrons travel along two beam lines towards the two experimental areas along : EAR-1 flight length of 185 m [4] (horizontal) and EAR-2 flight length of 19 m [5] (vertical). The neutron flux is larger in the EAR-2 and the energy resolution is better in the EAR-1.

The samples have been measured in both experimental areas. The measurement in EAR-2 has been done with three  $\text{C}_6\text{D}_6$  detectors and the Total Energy Detection (TED) [6] technique, and the measurement in EAR-1 with the n\_TOF Total Absorption Calorimeter (TAC) [7], designed to detect the complete  $\gamma$ -ray cascade. Measuring in both experimental areas with different detectors and techniques will allow to crosscheck results and, presumably, to reduce the final uncertainties.

The targets used for the experiment consist in two samples of  $^{244}\text{Cm}$  and one of  $^{246}\text{Cm}$ . There were 0.4 mg of  $^{244}\text{Cm}$  in each of the  $^{244}\text{Cm}$  samples and 1.1 mg of  $^{246}\text{Cm}$  in the  $^{246}\text{Cm}$  sample. The isotopic abundances of the different actinides are presented in Table 1.

**Table 1.** Isotopic composition (% atoms) of the  $^{244}\text{Cm}$  and  $^{246}\text{Cm}$  samples.

	$^{244}\text{Cm}$ sample	$^{246}\text{Cm}$ sample
$^{244}\text{Cm}$	$60.3\pm 1.1$	$20.3\pm 0.5$
$^{245}\text{Cm}$	$2.4\pm 0.3$	$1.1\pm 0.3$
$^{246}\text{Cm}$	$6.3\pm 0.6$	$57.7\pm 1.5$
$^{247}\text{Cm}$	-	$2.8\pm 0.4$
$^{248}\text{Cm}$	-	$8.8\pm 0.2$
$^{240}\text{Pu}$	$31.0\pm 0.6$	$9.3\pm 0.2$

### 2.1 Measurement at the EAR-2

The three  $\text{C}_6\text{D}_6$  detectors were placed at 5 cm from the sample and perpendicular to the beam. In addition, three additional detectors were used for monitoring the beam. Two of

them measured the intensity of the proton beam. The third one was the SiMon [8], an array of four silicon detectors facing a thin enriched lithium fluoride foil, for monitoring the neutron beam.

To obtain accurate weighting functions required for the PHWT [9] technique, a very detailed description of the experimental set-up has been implemented in the Geant4 toolkit [10]. The simulated response functions have been validated with experimental data obtained with several calibration sources ( $^{133}\text{Ba}$ ,  $^{137}\text{Cs}$ ,  $^{60}\text{Co}$ ,  $^{88}\text{Y}$ , AmBe and CmC). The geometry implemented in Geant4 and one of the simulated response functions are shown in Figure 1. The data obtained at n\_TOF are processed with the Pulse Shape Analysis (PSA) routine [11].

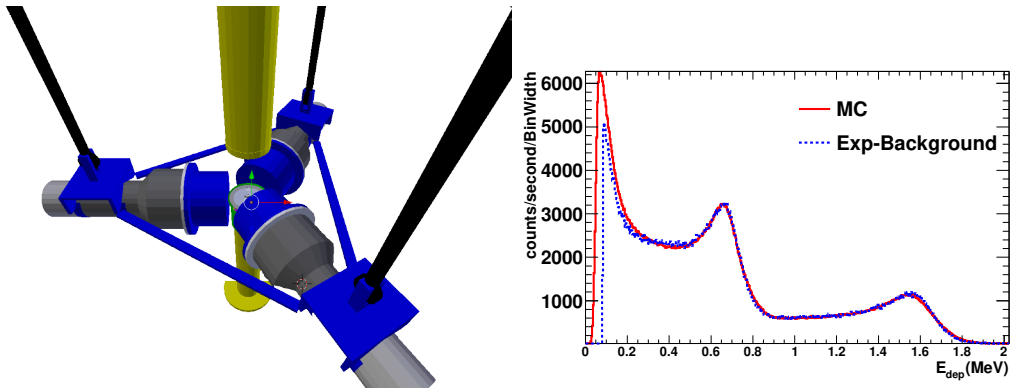


**Figure 1.** Geometry of the EAR-2 setup as implemented in Geant4 (left). Comparison between simulated (MC) and experimental response function to an  $^{88}\text{Y}$  source (right).

The results of the fits are stored in ROOT files [12]: signal amplitudes, signal areas, times, etc.. Also the conversion from time-of-flight to neutron energy is done.

Accurate amplitude-to-energy calibrations and gain stability checks were performed on a weekly basis for the three  $\text{C}_6\text{D}_6$  detectors using  $^{133}\text{Ba}$ ,  $^{137}\text{Cs}$ ,  $^{60}\text{Co}$ ,  $^{88}\text{Y}$ , AmBe and CmC calibration sources. Small gain shifts (8%) are observed and corrected as a function of time.

The total number of counts as a function of neutron energy measured with the Cm samples in place are shown in Figure 2. Also shown are the estimated total background, the beam related background, and the no-beam related background. These backgrounds have been obtained from dedicated measurements.

A preliminary but rather complete analysis of the data measured at the EAR-2 has been performed and two preliminary capture yields (no background subtracted) have been obtained, one for the  $^{244}\text{Cm}$  samples and the other for the  $^{246}\text{Cm}$  sample. Both yields (no background subtracted) are presented in Figure 3 together with the yields obtained from the JEFF-3.3 [13] cross sections with the experimental background and the characteristics of the EAR-2 neutron beam (neutron flux + *resolution function*)[14]. The relative differences between the experimental and the evaluated yields (in %) are shown at the bottom of each panel, integrated for each resonance. The results have been normalized to the first large resonance of  $^{240}\text{Pu}$  at 1 eV.

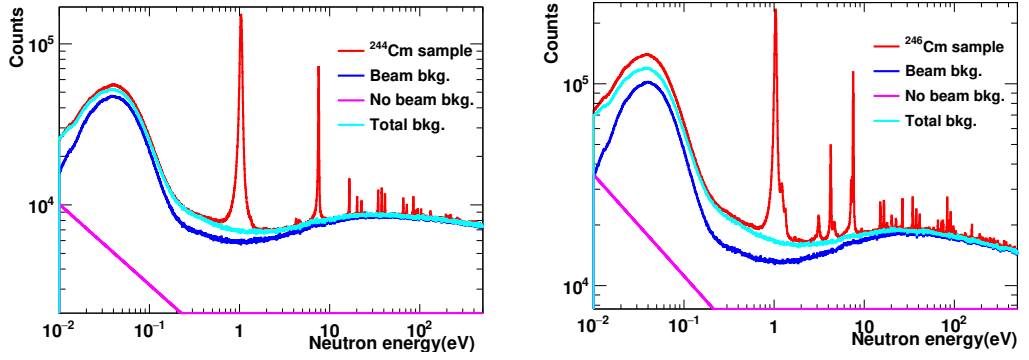


**Figure 2.** Total number of counts (750 bins per decade) and estimated backgrounds registered in the  $^{244}\text{Cm}$  (left) and  $^{246}\text{Cm}$  (right) EAR-2 measurements.

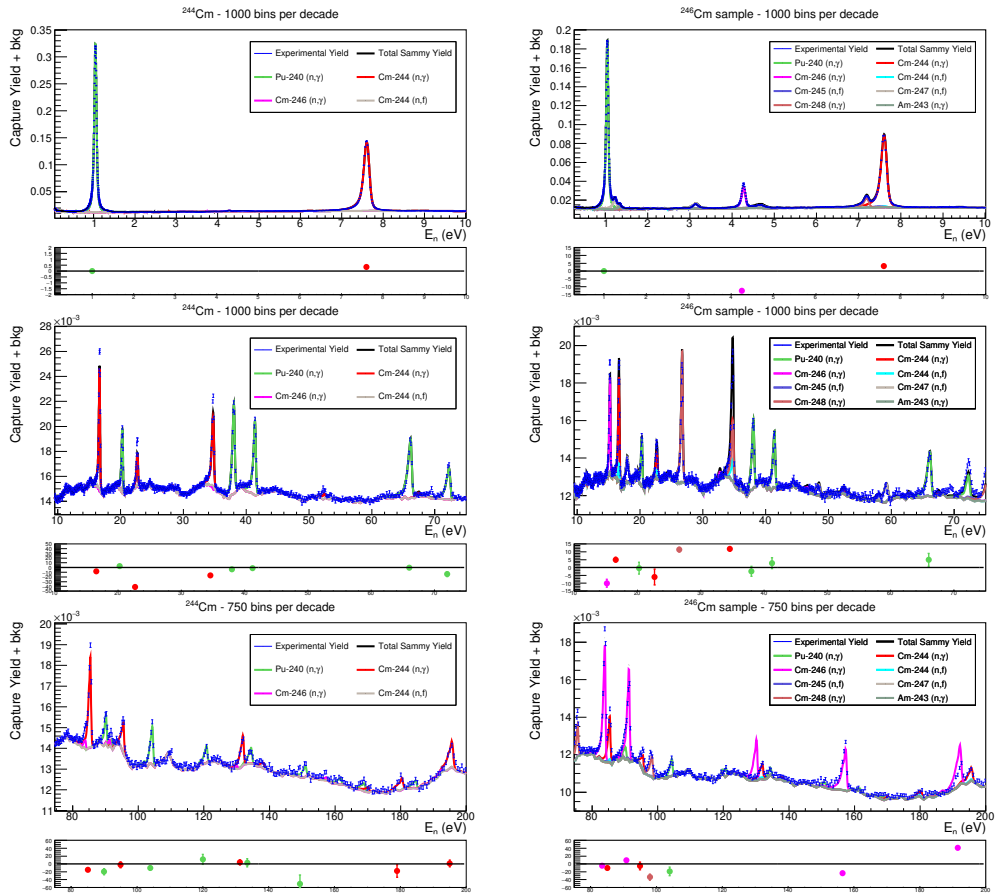


**Figure 3.** Preliminary experimental yields (no background subtracted) of the measured  $^{244}\text{Cm}$  (left) and  $^{246}\text{Cm}$  (right) samples. Together with the experimental data points, we show an estimation of the contribution of the capture and fission reactions in each isotope present in the samples. These contributions have been obtained using the SAMMY computer code to calculate the reaction yields taking into account the experimental conditions such as Doppler and resolution broadening, and taking the reaction cross sections from JEFF-3.3. The resulting yields were then normalized to fit the experimental results and added to the background, obtained from dedicated measurements.

## 2.2 Measurement at the EAR-1

The measurement in EAR-1 was performed with the TAC, which is an array of 40 BaF<sub>2</sub> crystals designed to detect the full capture  $\gamma$ -ray cascades. The data analysis is ongoing and it will follow similar procedures than the ones performed in previous TAC experiments [15] [16]. Signals are grouped into TAC events with a 20 ns coincidence window, and cuts in total deposited energy and detection multiplicity allow to improve the signal to background ratio.

The total number of counts as a function of neutron energy measured with the <sup>244</sup>Cm samples in place are shown in Figure 4, together with the estimated backgrounds. The better energy resolution and smaller instantaneous neutron fluence in EAR-1 results in a narrower resonant structure and a larger contribution of the no-beam related background.

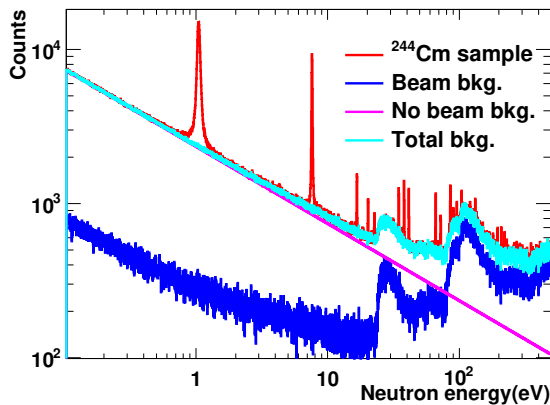


**Figure 4.** Total number of counts (1000 bins per decade) and estimated backgrounds registered in the <sup>244</sup>Cm EAR-1 measurement.

## 3 Conclusions

The capture cross sections of <sup>244</sup>Cm and <sup>246</sup>Cm are required to estimate the production and transmutation rates of MAs in LWR and also for new reactor types. There are only two previous capture measurements of these two isotopes, both of them with many experimental difficulties. Therefore, a new measurement has been performed at n\_TOF using the two experimental areas and preliminary capture yields have been obtained.

## References

- [1] M. S. Moore et. al., Phys. Rev. C, 3, 1656 (1971)
- [2] A. Kimura et. al., Jour. Nucl. Sc. Tech. 49, 708 (2012)
- [3] G. Aliberti et. al., Ann. Nucl. Ener. 33, 700 (2006)
- [4] C. Guerrero et al., Eur. Phys. J. A 49, 27 (2013)
- [5] C. Weiss et al., Nucl. Instrum. Meth. A 799, 90 (2015)
- [6] R.L. Macklin and J.H. Gibbons, Phys. Rev. 159, 1007 (1967)
- [7] C. Guerrero et al., Nucl. Instrum. Meth. A 608, 424 (2009)
- [8] S. Marrone et al., Nucl. Instrum. Meth. A 517, 389 (2004)

- [9] Abondano et al., Nucl. Instrum. Meth. A 521, 454 (2004)
- [10] S. Agostinelli et al., Nucl. Instrum. Meth. A 506, 250 (2003)
- [11] P. Žugec et al., Nucl. Instrum. Meth. A 812, 134 (2016)
- [12] <https://root.cern.ch/>
- [13] A. Koning et al., J. Korean Phys. Soc. 59, 1057 (2011); The JEFF library is available from <https://www.oecd-nea.org/dbdata/jeff>
- [14] M. Sabaté-Gilarte et al., Eur. Phys. J 53, 10 (2017)
- [15] C. Guerrero et al., Phys. Rev. C 85, 044616 (2012)
- [16] E. Mendoza et al., Phys. Rev. C 90, 034608 (2014)